

critical velocity goes to zero. If one uses their formula for  $E$  when a vortex is near the wall [their Eq. (14)], but uses the value  $I_1$  [Eq. (8)] which assumes that the vortex was created at the wall, then the limiting value of  $E/I_1$  for a ring at the wall is  $\kappa/2\pi a \approx 1.6 \times 10^4$  cm/sec for  $\kappa = h/m$  and  $a$  (the core radius) =  $10^{-8}$  cm. As pointed out by Vinen, this eliminates the problem, even classically, that the critical velocity for the creation of vortex rings at the wall is predicted to be zero. However, the value  $\kappa/2\pi a$  is a maximum value of  $E/I_1$  for rings near the wall and should not represent a critical velocity.

In a quantum calculation Fetter<sup>9</sup> showed that the energy of a ring does not go to zero as it approaches the wall. If one does the injustice of dividing the quantum value of  $E$  by the classical value  $I_1$ , one gets  $E/P \rightarrow (11/12)\kappa/8\pi b$ , where  $b$  is the distance from the ring to the wall. Again this is a maximum as  $b \rightarrow 0$ , but the result is not meaningful since  $I_1$  should also be calculated quantum mechanically. Because the impulse required to create a ring is not unique, some care should be exercised before one substitutes  $I$  for  $P$  in Landau's formula.

The author wishes to thank Dr. E. Hammell,

Dr. W. Keller, Professor B. Sonnerup, and Professor J. N. Kidder for helpful discussion on hydrodynamics.

<sup>1</sup>H. Lamb, Hydrodynamics (Dover Publications, New York, 1945), Sec. 152.

<sup>2</sup>C. C. Lin, in Liquid Helium, Proceedings of the Enrico Fermi International School of Physics, Course XXI, edited by G. Careri (Academic Press, Inc., New York, 1963) p. 99.

<sup>3</sup>Yu. G. Mamaladze, in Proceedings of the Ninth International Conference on Low Temperature Physics, edited by J. G. Daunt, D. O. Edwards, F. J. Milford, and M. Yaquob (Plenum Press, New York, 1965), pp. 281-283.

<sup>4</sup>W. F. Vinen, in Quantum Fluids, edited by D. F. Brewer (North-Holland Publishing Company, Amsterdam, 1966), pp. 104-106.

<sup>5</sup>J. C. Fineman and C. E. Chase, Phys. Rev. **129**, 1 (1963).

<sup>6</sup>Lin, Ref. 2, Eq. (1.A5).

<sup>7</sup>For a clear discussion of this method, see R. W. Sears, Theoretical Aerodynamics, Pt. 1: Introduction to Theoretical Hydrodynamics (Graduate School of Aeronautical Engineering, Cornell University, Ithaca, New York, 1957), pp. 4.16-4.24.

<sup>8</sup>G. W. Rayfield and F. Reif, Phys. Rev. **136**, A1194 (1964); see p. A1201.

<sup>9</sup>A. L. Fetter, Phys. Rev. **138**, A429 (1965).

## INFRARED OPTICAL PROPERTIES OF VANADIUM DIOXIDE ABOVE AND BELOW THE TRANSITION TEMPERATURE

A. S. Barker, Jr., H. W. Verleur, and H. J. Guggenheim

Bell Telephone Laboratories, Murray Hill, New Jersey

(Received 1 November 1966)

We have measured the infrared reflection and transmission spectra of crystals of  $\text{VO}_2$  both above and below its transition temperature  $T_t = 68^\circ\text{C}$ . Since the work of Morin<sup>1</sup> which showed the transition as an abrupt change of resistance there have been many recent speculations on the nature of the transitions in  $3d$  transition-metal oxides<sup>2,3</sup>: whether they are metallic  $\leftrightarrow$  antiferromagnetic, and/or metallic  $\leftrightarrow$  semiconducting, and whether the conduction in the more insulating state below  $T_t$  is band-type or hopping-type. In a recent communication Adler<sup>4</sup> has discussed a model for  $\text{Ti}_2\text{O}_3$  with a gap which goes rapidly to zero at  $T_t$  because of an exchange interaction. A somewhat different model<sup>5</sup> gives a rapidly disappearing gap as a result of a crystalline struc-

ture distortion. We have investigated the conduction properties using analysis of infrared reflection and transmission, and we present the first Hall data in  $\text{VO}_2$  both above and below  $T_t$ . We have also examined the question of lattice stability and conclude that there is not a Cochran-type ferroelectric mode<sup>6</sup> connected with the transition. The crystals used were grown by decomposing  $\text{V}_2\text{O}_5$  in a temperature-difference system. Chemical analysis showed the stoichiometry to be  $\text{VO}_x$  with  $x = 2.01 \pm 0.01$ .

Group theory applied to monoclinic ( $m$ )  $\text{VO}_2$  shows that in the long-wavelength limit there are eight infrared-active modes for the electric vector  $\vec{E}$  parallel to the  $b_m$  axis and seven infrared-active modes for  $\vec{E}$  in the plane perpendicular to the  $b_m$  axis. In addition, there

are 18 Raman-active modes. In  $\text{VO}_2$  for  $T > T_t$  (rutile structure  $r$ ) there are three infrared-active modes perpendicular to the  $c_r$  axis and one parallel to the  $c_r$  axis.

The reflectivity spectra were measured in the usual manner<sup>7</sup> both below and above  $T_t$ , as well as at a temperature near  $T_t$ . The range of frequencies covered was from 100 to 20 000  $\text{cm}^{-1}$ . The spectra at room temperature were measured with all possibly distinct orientations of the crystal. However, distinct spectra were obtained only with  $\vec{E}$  parallel or perpendicular to the  $a_m$  axis. Figure 1 shows the  $E \parallel a_m$  spectra. The lack of a unique  $E \parallel b_m$  spectrum below  $T_t$  leads to an interesting conclusion concerning the crystal structure. At  $T_t$ , the crystallographic transformation is<sup>8</sup>

$$a_m \rightarrow 2c_r, \quad b_m \rightarrow a_r, \quad c_m \rightarrow a_r - c_r.$$

Furthermore, the distortion is slight, so that  $|c_m|_T < T_t \approx |a_r - c_r|_T > T_t$ . If one views the crystal in the low-temperature phase in reflection using a polarizing microscope, one observes

a domain pattern.<sup>9</sup> The reflectivity measurements suggest that these domains are the result of the monoclinic  $b_m$  axis choosing one  $a_r$  axis to point along in one region and choosing the other  $a_r$  axis in another region when the crystal is cooled through  $T_t$ . Typical domains are about 40  $\mu$  across the narrow dimension; thus we have not been able to measure the reflectivity spectrum of a single domain.

We have used the classical oscillator expression for  $\epsilon$ , the dielectric function, to fit the reflectivity spectra below and above  $T_t$ . The oscillator parameters for  $E \parallel a_m$  and  $E \perp a_m$  are listed in Table I. We have fitted nine modes to the  $E \parallel$  spectrum. We assume that the highest frequency "mode" simulates the band-to-band transitions. Newman, Lawson, and Brown<sup>3</sup> have observed an activation energy in conductivity measurements of 4000  $\text{cm}^{-1}$ , suggesting a gap at 8000  $\text{cm}^{-1}$ . However, activation energies as low as 1600  $\text{cm}^{-1}$  have also been observed.<sup>10</sup> Preliminary transmission measurements on our single-crystal samples show an onset of absorption near 2500  $\text{cm}^{-1}$  which may

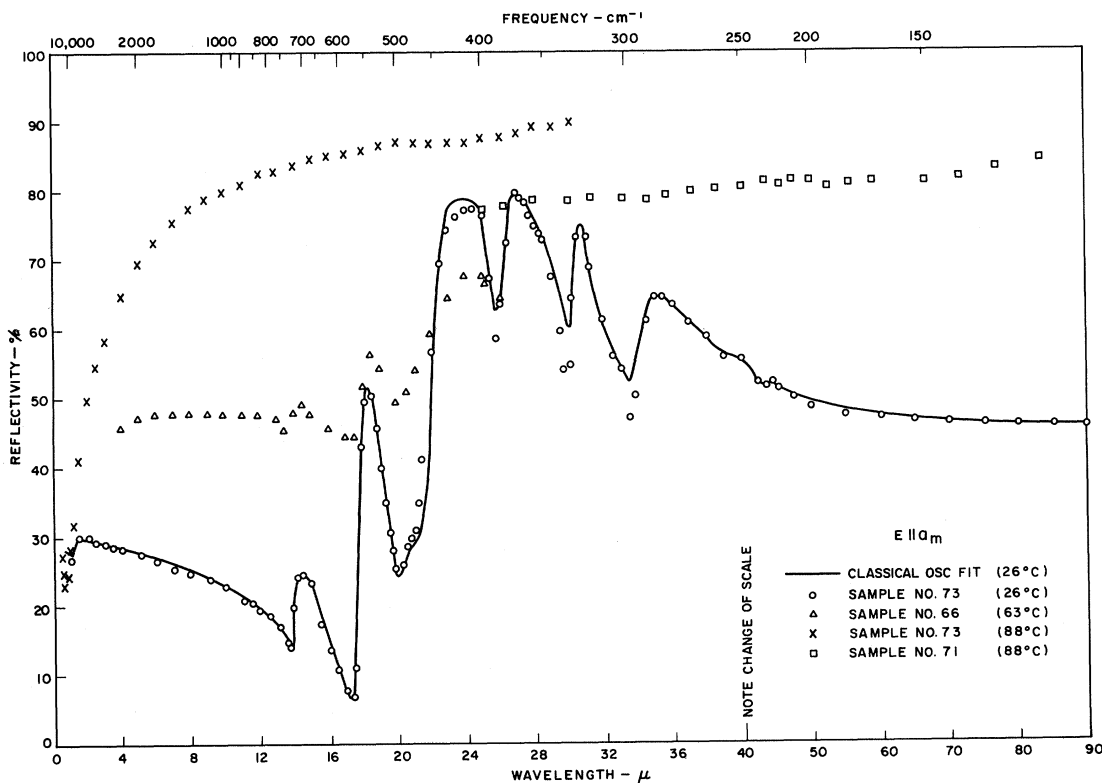


FIG. 1. Reflectivity of  $\text{VO}_2$ . The solid curve is a fit for  $T < T_t$  using eight phonon modes and one band-structure mode. The crosses and squares show the data above  $T_t$ . The squares are low because of sample cracking; however, they illustrate the monotonic rise expected of free carrier reflection. The triangle points were taken on cooling. Because of thermal hysteresis,  $T_t \approx 63^\circ\text{C}$  for this run.

Table I. VO<sub>2</sub> classical oscillator parameters for the dielectric function above and below  $T_t$ .

Mode no.	$\omega$ (cm <sup>-1</sup> )	$E \perp a_m$		$E \parallel a_m$		
		$4\pi\rho$	$\gamma$	$\omega$ (cm <sup>-1</sup> )	$4\pi\rho$	$\gamma$
$T = 26^\circ\text{C}$ , primitive cell V <sub>4</sub> O <sub>8</sub> (monoclinic)						
1	189	0.54	0.012	227.5	0.1	0.02
2	270	13.0	0.07	285	3.3	0.06
3	310	7.0	0.05	324	1.95	0.018
4	340	0.7	0.024	355	7.4	0.08
5	505	3.1	0.07	392.5	1.0	0.03
6	600	4.8	0.074	478	0.2	0.08
7	710	0.15	0.06	530	0.65	0.045
8	10 000	1.3	0.4	700	0.25	0.055
9				10 000	1.3	0.4
$\epsilon_\infty = 10.0$ , $\epsilon_0 = 40.6$			$\epsilon_\infty = 9.7$ , $\epsilon_0 = 25.9$			
$T = 80^\circ\text{C}$ , primitive cell V <sub>2</sub> O <sub>4</sub>						
$E \parallel c_r$ (rutile)						
$\omega_p = 8000 \text{ cm}^{-1}$ , $\omega_c = 10\,000 \text{ cm}^{-1}$ , $\epsilon_\infty = 9$						

be the band gap. The remaining optical phonon modes have strengths typical of ionic crystals.

Because of the domain problem, the  $E \perp a_m$  spectra can exhibit up to 15 optical phonon modes with strengths which depend on the angle between the  $E$  vector and the dipole moment of the normal modes, some of which lie along  $b_m$  and some of which are perpendicular to  $b_m$ . While there is much fine structure, the data are adequately fit by the seven modes listed in Table I plus a band-structure mode near  $10\,000 \text{ cm}^{-1}$  similar to that for  $E \parallel a_m$ . Neither polarization shows a strong low-frequency mode such as might be expected if the transition were caused by a Cochran-type infrared-active mode, though such a mode may exist above  $T_t$  and change its character completely below  $T_t$ . We note, however, that the ion shifts<sup>8</sup> at  $T_t$  are typical of a  $(101)_r$  or a  $(011)_r$  zone-boundary phonon and thus not likely to show up even for  $T > T_t$  in the first-order spectrum.

Figure 1 shows a typical reflectivity spectrum for  $T > T_t$ . Two samples were used for this run. After the long-wavelength data were taken, the sample appeared to be cracked, which probably caused the discontinuity between the low- and the (more reliable) high-frequency measurements. The spectra for all other polarizations with  $T > T_t$  show similar high reflectivity typical of metallic or free carrier behavior, except that the reflectivity spectrum for  $E \perp c_r$  (not shown) has some additional structure near  $660 \text{ cm}^{-1}$ . We hesitate to interpret

this as being due to an optical phonon in the rutile phase because it was not reproduced in all other crystals we measured.

We list in Table I the dielectric-function parameters  $\omega_p$  and  $\omega_c$ , the plasma and collision frequencies, where  $\epsilon(\text{carriers}) = -\omega_p^2 \epsilon_\infty / (\omega^2 - i\omega\omega_c)$  for one  $E \parallel c_r$  spectrum. For  $T \simeq T_t$  we see both the semiconducting-phase phonons and the metallic-phase phonons and the metallic-phase plasma. We interpret this spectrum (Fig. 1) as arising from the coexistence of regions of both phases. Table II shows the Hall effect data on samples from the same growth batch as those studied in the infrared. The only measurement of a Hall voltage detectable above noise (for  $T > T_t$ ) gives  $n \sim 30 \times 10^{20}$  electrons/cm<sup>3</sup>. This represents only 0.1 electron per vanadium ion and raises the question of whether we actually have simple "metallic" conductivity. Proceeding, however, and using  $n \sim 30 \times 10^{20}$  combined with the infrared results, we deduce an optical mass of  $m^* \sim 0.5m_e$  and an optical mobility of  $\mu_{\text{opt}} = e/\omega_c m^* \sim 2 \text{ cm}^2/\text{V sec}$  for the metallic phase.

The d.c. mobility in the semiconducting phase (Table II), though small, is many orders of magnitude larger than in NiO, a hopping-type conductor.<sup>11</sup> Rough fits to the infrared free-carrier absorption measured by transmission at  $25^\circ\text{C}$  in the  $1000$ - to  $5000\text{-cm}^{-1}$  region combined with the Hall measurements suggest that  $m^*$  is greater than  $m_e$ , and may be as large as  $4m_e$ . Recent nuclear magnetic resonance

Table II. Hall effect and resistivity of VO<sub>2</sub>.

Sample	Temperature (°C)	Current direction	$\rho$ ( $\Omega$ cm)	$n = 1/R_H c$ ( $10^{20}$ cm <sup>-3</sup> )	$\mu$ (cm <sup>2</sup> /V sec)
78	22	$\perp a_m$	1	0.09 <sup>a</sup>	0.7
78	80	$\perp c_\gamma$	0.000 14	>23	>19
80	22	$\perp a_m$	1.2	0.09 <sup>a</sup>	0.6
80	81	$\perp c_\gamma$	0.000 24	>17	>15
80	22	$\parallel a_m$	1.4	0.086 <sup>a</sup>	0.52
80	79	$\parallel c_\gamma$	0.000 13	$\sim 30^{a,b}$	$\sim 16^b$

<sup>a</sup>Hall voltage corresponds to electrons.

<sup>b</sup>Factor of 2 uncertainty.

measurements<sup>12</sup> show that VO<sub>2</sub> does not become antiferromagnetic at  $T_t$ . Our crystals show a constant magnetic susceptibility of  $0.88 \times 10^{-6}$  emu/g from room temperature down to 100°K, where a Curie-law behavior sets in ( $T_C \sim 0^\circ\text{K}$ ) which may be due to impurities. It appears then that a gap opens up on cooling through  $T_t$  causing a transition to a nonmagnetic semiconducting phase.

The authors wish to thank G. E. Smith and D. A. Kleinman for helpful conversations and R. C. Sherwood for measuring the magnetic susceptibility.

<sup>1</sup>F. J. Morin, Phys. Rev. Letters **3**, 34 (1959); see also Semiconductors, edited by N. B. Hannay (Rein-

hold Publishing Corporation, New York, 1959), Chap. 14.

<sup>2</sup>T. Kawakubo, J. Phys. Soc. Japan **20**, 516 (1965).

<sup>3</sup>C. H. Neuman, A. W. Lawson, and R. F. Brown, J. Chem. Phys. **41**, 1591 (1964).

<sup>4</sup>David Adler, Phys. Rev. Letters **17**, 139 (1966).

<sup>5</sup>David Adler and Harvey Brooks, Phys. Rev., to be published.

<sup>6</sup>W. Cochran, Advan. Phys. **9**, 387 (1960).

<sup>7</sup>W. G. Spitzer and D. A. Kleinman, Phys. Rev. **121**, 1324 (1961).

<sup>8</sup>Georg Andersson, Acta. Chem. Scand. **10**, 623 (1956).

<sup>9</sup>P. J. Fillingham and H. J. Guggenheim, private communication.

<sup>10</sup>H. Takei and S. Koide, J. Phys. Soc. Japan **21**, 1010 (1966).

<sup>11</sup>D. P. Snowden and H. Saltsburg, Phys. Rev. Letters **14**, 497 (1965).

<sup>12</sup>J. Umeda, H. Kusumoto, K. Narita, and E. Yamada, J. Chem. Phys. **42**, 1458 (1965).